

1

1

2

3 Technical note: Large offsets between different datasets of sea-water
4 isotopic composition:

5 an illustration of the need to reinforce intercalibration efforts

6

7

8 Gilles Reverdin¹, Claire Waelbroeck¹, Antje H. L. Voelker^{2,3}, Hanno Meyer⁴

9

10

11

12 ¹ Laboratoire LOCEAN/IPSL, Sorbonne Université-CNRS-IRD-MNHN, Paris, 75005,
13 France

14 ² Instituto Português do Mar e da Atmosfera (IPMA), Algés, Portugal

15 ³ Center of Marine Sciences (CCMAR), Universidade do Algarve, Faro, Portugal

16 ⁴ Alfred Wegener Institute Potsdam, 14473 Potsdam, Germany

17

18 Corresponding author: Gilles Reverdin gilles.reverdin@locean.ipsl.fr

19

Code de champ modifié

20 Abstract

21 We illustrate offsets in surface seawater isotopic composition between recent, public
22 data-sets from the Atlantic Ocean and the subtropical ~~Southe-Eastern~~ Indian Ocean. The
23 observed offsets between data-sets often exceed 0.10‰ in $\delta^{18}\text{O}$ and 0.50‰ in $\delta^2\text{H}$. They
24 might in part originate from different sampling of seasonal, interannual or spatial
25 variability. However, they likely mostly originate from different instrumentations and
26 protocols used to measure the water samples. Estimation of the systematic offsets is
27 required before merging the different data-sets in order to investigate spatio-temporal
28 variability of isotopic composition in the world ocean surface waters. This highlights the
29 need to actively share seawater isotopic composition samples dedicated to specific
30 intercomparison of data produced in the different laboratories and to promote best
31 practices, a task to be addressed by the new SCOR working group 171.

32

33

34 1. Introduction

35 Seawater isotopic composition ($^{18}\text{O}/^{16}\text{O}$ and $^2\text{H}/^1\text{H}$ ratios expressed as $\delta^{18}\text{O}$ and $\delta^2\text{H}$ in
36 ‰ in the VSMOW/SLAP scale) is classified as an Essential Ocean/Climate Variable
37 (EOV/ECV) in international programs such as GEOTRACES and GO-SHIP. Stable
38 seawater isotopes ($\delta^{18}\text{O}$, $\delta^2\text{H}$) are used to trace sources of freshwater (precipitation,
39 evaporation, runoff, melting glaciers, sea ice formation and melting), both at the ocean
40 surface and in the ocean interior (Schmidt et al., 2007; Hilaire-Marcel et al., 2021).
41 Except for fractionation during phase changes, the water isotopic composition is nearly
42 conservative in the ocean.

43 A major emphasis is on high latitude oceanography. There, continental (or iceberg)
44 glacial melt, formation or melt of sea ice, and high-latitude river inputs (for the Arctic)
45 leave imprints on the surface ocean isotopic composition, as well as below the surface
46 down to 800 m close to ice shelves in the Southern Ocean (Randall-Goodwin et al.,
47 2015; Biddle et al., 2019, Hennig et al., 2024). In contrast, few studies have been
48 performed on the isotopic signature in the deep ocean (e.g., Prasanna et al., 2015;
49 Voelker et al., 2015). Seawater isotopes in the upper ocean at low latitudes are often
50 vital for paleoclimatic studies, as they are needed to calibrate proxies of past ocean
51 variability in marine carbonate records such as corals and foraminifera (e.g., PAGES
52 CoralHydro2k working group; Konecky et al., 2020). Seawater isotopes are also
53 important tracers in the coastal ocean, with emphasis on upwelling (Conroy et al., 2014,
54 2017; Kubota et al., 2022; Lao et al., 2022), and river discharges (e.g., Amazon) (Karr and
55 Showers, 2001). Surface ocean seawater isotopes are also used to characterize
56 evaporation rates and air-sea interactions (Benetti et al., 2017).

57 The isotopic signatures of these different processes are evolving in our warming world,
58 which will imprint on the seawater isotopic composition (Oppo et al., 2007).
59 Additionally, seawater isotope data provide model boundary conditions and allow the
60 assessment of model performance in isotope-enabled Earth system models (e.g. Schmidt
61 et al., 2007; Brady et al., 2019; Cauquoin et al., 2019), thereby improving climate model
62 projections of the future.

63 Stable seawater isotope data have thus been massively produced in the last decades by
64 a variety of methods. For example, most data compiled in the "GISS Global Seawater
65 Oxygen-18 Database -V1.21" for stable seawater isotopes (LeGrande and Schmidt, 2006)
66 originate from Isotope-ratio Mass Spectrometry (IRMS). They were mostly measured in
67 earlier decades by dual-inlet technology (highest precision), whereas, more recently, the
68 continuous-flow method (lower precision) became widespread for seawater isotope
69 analysis. In the last decade, cavity ring-down spectroscopy (CRDS) turned into another
70 commonly used method as it allows parallel measurement of $\delta^{18}\text{O}$ and $\delta^2\text{H}$, but with
71 often lower precision, at least early on (e.g., Voelker et al., 2015).

72 Reverdin et al. (2022) recently compiled a mix of data produced by IRMS and CRDS at
73 LOCEAN (<https://www.seanoe.org/data/00600/71186/>). As CRDS and other laser
74 techniques (Glaubke et al., 2024; [hereafter GWS2024](#)) have become more prevalent
75 recently, they contribute a significant part of the new data produced and thus also to the
76 soon to be released CoralHydro2k seawater database for $\delta^{18}\text{O}$ ($\delta^2\text{H}$) ~~(with a focus on the~~
77 ~~tropics (35°N-35°S))~~ (Atwood et al., 2024).

78 There are potential differences between the data produced by the two methods.
79 Typically, CO_2 -water or H_2 -water equilibration was used for the IRMS measurements
80 and yields measurements of the activity of water, which decreases with increasing
81 salinity. Furthermore, concentration of divalent cations like Mg^{++} are responsible
82 for slight changes in fractionation factors. On the other hand, the laser methods such as
83 CRDS evaporate the entire sample. If the samples have not been distilled beforehand,
84 there is an issue of salt deposition and of resulting absorption or desorption of water
85 with fractionation effects. In the LOCEAN database (Reverdin et al., 2022), an attempt
86 was made to adjust the data, based on the analysis of Benetti et al (2017b). This was also
87 adopted by at least one other group (Haumann et al., 2022), but overall, there is the
88 possibility of an offset of these data with respect to the ones of other groups using CRDS.
89 However, it should be noted that some studies reporting unadjusted $\delta^{18}\text{O}$ measurements
90 from CRDS and IRMS technique with CO_2 -water equilibration provide data that were
91 undistinguishable within instrumental precision (Walker et al., 2016; Hennig et al.,
92 2024).

Code de champ modifié

93 It is actually quite common when using water isotope data in studies involving more
94 than one data-set, to first evaluate whether there are possible offsets. Intercomparison
95 with earlier data or reference materials was a prerequisite for GEOTRACES sampling
96 campaigns, although for the water isotopes this was, unfortunately, seldomly followed
97 (e.g., Voelker et al., 2015). These intercomparisons often outline systematic differences
98 which could result from the issue outlined above, or from other issues, such as
99 uncertainties in reference materials used, analysis protocols, or isotopic changes in the
100 samples during their handling and storage (Benetti et al., 2017a; Akhoudas et al., 2019;
101 Hennig et al., 2024). In other cases, this was not done, either because the data stood by
102 themselves (Bonne et al., 2019, for $\delta^{18}\text{O}$ and $\delta^2\text{H}$ data), or there was no comparison data
103 available in the same region (Glaubke et al., GWS-2024, for $\delta^{18}\text{O}$ data). The possible
104 offsets can however become an issue, when these data are placed in a larger context. For
105 example, Glaubke et al. (GWS2024) identify a large difference in the S- $\delta^{18}\text{O}$ relationship
106 in the subtropical Indian Ocean between their data in the south-eastern part and other
107 data in the south-western Indian Ocean. They also discuss and question differences in
108 the deep water-masses isotopic values between separate data-sets, but as these might
109 also be explained by large uncertainties in these data, we will not address them further.

110 Using these two examples (Bonne et al., 2019; Glaubke et al., GWS 2024), the aim of this
111 note is to point out the interest when producing a new data-set, of exchanging collected
112 samples to carry a direct comparison, or, if this was not done, to compare the data with
113 other published data and evaluate potential systematic differences.

114 2. Comparisons

115 For identifying possible offsets, we consider surface ocean subsets of the LOCEAN data
116 base in specific regions for roughly the same years as the other data collected. The data
117 extracted are from the same regions as in the datasets of the two studies and are
118 gathered in S- $\delta^{18}\text{O}$ space as well as in S- $\delta^2\text{H}$ space (~~available only presented only~~ for the
119 Bonne et al (2019) data-set), where S is reported as a practical salinity with the practical
120 salinity scale of 1978 (~~psa~~). The assumption done here as in many papers is that the S-
121 $\delta^{18}\text{O}$ relationship holds on fairly large scales in the surface layer (for the eastern
122 subtropical North Atlantic, see for example, the discussion in Voelker et al (2015) and in
123 Benetti et al. (2017a)). Obviously, this has limitations, such as in areas influenced by

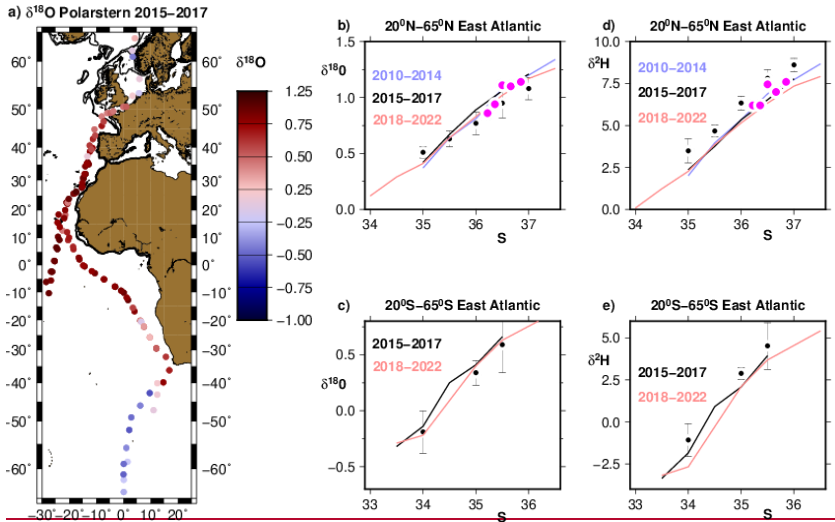
124 more than one water mass or by multiple freshwater end-members (meteoric,
125 continental run-off, sea ice melt or formation, evaporation).

126 2.1 Daily surface data collected from R.V. Polarstern

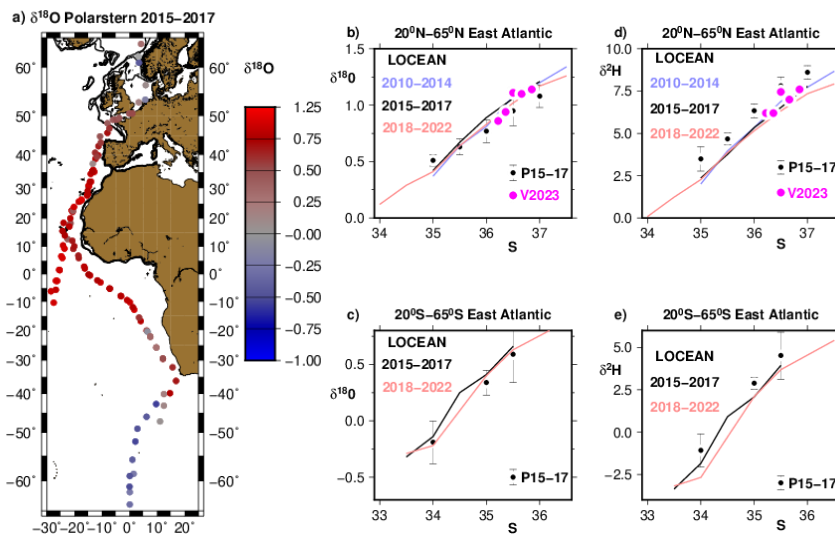
127 The surface seawater samples originated from daily collection during two years on
128 board RV Polarstern in 2015-2017 (Bonne et al., 2019). There is no salinity provided
129 with the data, and here we chose to associate them with the simultaneously collected
130 thermosalinograph (TSG) data collected on board the RV Polarstern and available from
131 PANGAEA (for each cruise, an indexed file with title starting by 'Continuous
132 thermosalinograph oceanography along Polarstern' is included in PANGAEA: for example,
133 TSG data for the first cruise (PS90) associated with the isotopic seawater data are found
134 at <https://doi.org/10.1594/PANGAEA.858885>). The water samples were not collected
135 from the same water line and pumping depth as the TSG data, which can result in
136 differences. This is however likely to be small in most circumstances away from large
137 freshwater input at the sea surface, such as from melting sea ice, intense rainfall and
138 river estuaries (Boutin et al., 2016). We also applied an adjustment of +0.25‰ to the
139 $\delta^{18}\text{O}$ data of Bonne et al. (2019), based on post-analysis identification of a bias in an
140 internal reference material.

141 We then estimate averages of all the data as a function of salinity in two domains
142 extending poleward of the subtropical salinity maximum toward the higher latitudes in
143 the eastern part of the Atlantic Ocean (thus, 20°N to 65°N and the same in the southern
144 hemisphere). This is done by sorting out the data by salinity classes of 0.5. The LOCEAN
145 data until 2016 in the North and tropical Atlantic were presented ~~by~~ Benetti et al
146 (2017a), showing the tightness of the S- $\delta^{18}\text{O}$ and S- $\delta^2\text{H}$ relationships in vast domains of
147 the eastern Atlantic. In the North Atlantic, LOCEAN data have been continuously
148 collected since 2011, and south of 10°S in the eastern Atlantic mostly since 2017.

Code de champ modifié



149



150

151

152

153 Figure 1: Comparison of the LOCEAN and Bonne et al. (2019) datasets. (a) map of RV
 154 Polarstern original-data-set points east of 30°W in the eastern Atlantic Ocean east of

Mis en forme : Anglais (États-Unis)

155 30°W. (b), (c), (d), (e) Water isotopes-S scatter diagrams averaged as a function of
156 salinity in 0.5 practical salinity bins (left (b) and (c) for $\delta^{18}\text{O}$, and right, (d) and (e) for
157 $\delta^2\text{H}$), top for the northern hemisphere and bottom for the southern hemisphere, east of
158 30°W and outside of [20°N, 20°S]. ~~The black dots with error bars are the binned~~
159 ~~averages of the Bonne et al. (2019) RV Polarstern data in 2015-2017 (after adjustment~~
160 ~~of +0.25‰ to $\delta^{18}\text{O}$) (P15-17), with the root mean square of the variance reported as~~
161 ~~error bars. Five individual surface points from Voelker et al (2023) (V2023) are also~~
162 ~~plotted (magenta dots).~~ The colored ~~curves-lines~~ represent average relationships of
163 water isotopes in the LOCEAN data base ~~in the same regions~~ as a function of practical
164 salinity for three different period ranges, ~~whereas the black dots with error bars are the~~
165 ~~binned averages of the Bonne et al. (2019) RV Polarstern data in 2015-2017 (after~~
166 ~~adjustment of +0.25‰ to $\delta^{18}\text{O}$), with the root mean square of the variance reported as~~
167 ~~error bars. Five individual surface points from Voelker et al (2023) are also plotted~~
168 ~~(magenta dots).~~

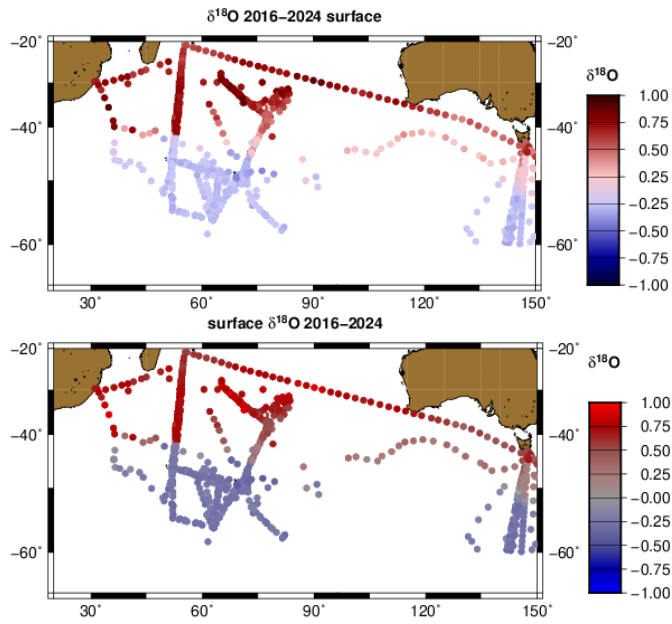
169 The average relationships found in the LOCEAN data-set for three periods overlay well
170 in particular in the northern hemisphere. Uncertainties on individual curves (not
171 shown) are estimated based on the scatter of individual data in each salinity bin. They
172 are typically on the order of 0.01-0.02 (0.05-0.10) ‰ for $\delta^{18}\text{O}$ ($\delta^2\text{H}$) respectively in the
173 northern hemisphere (top panel), and a little larger for the less sampled southern
174 hemisphere curves in 2015-2017. Sampling is usually also insufficient at the low end of
175 the salinity range, to reliably estimate an uncertainty. Thus, these different curves nearly
176 overlay within the sampling uncertainty. Five surface samples that were collected in the
177 Northeast Atlantic during the same years within the same salinity range (Voelker et al.,
178 2023), also fit well on the North Atlantic curves. The adjusted $\delta^{18}\text{O}$ data from Bonne et
179 al. (2019) are slightly shifted downward with respect to the curves (Fig. 1b, c), with the
180 plotted standard deviation of individual data around the average not overlapping the
181 LOCEAN data average curves in most cases for the same years 2015-2017. The situation
182 is opposite for the 35- salinity bin in the northern hemisphere, with the adjusted $\delta^{18}\text{O}$
183 data from Bonne et al. (2019) being above the three LOCEAN average curves, which
184 might be due to samples collected uniquely in the English Channel and North Sea by RV
185 Polarstern in this salinity range, whereas sampling is more geographically-spread in the
186 LOCEAN data base.

187 Altogether, the average $\delta^{18}\text{O}$ offset is small, with the LOCEAN data being higher by $0.02 \pm$
188 0.01 ‰ than the $\delta^{18}\text{O}$ from Bonne et al. (2019), which is not significantly different from
189 0 based on the interannual differences witnessed in the LOCEAN curves and the
190 scatter/uncertainty in the [RV Polarstern](#) data. A systematic difference is, however, found
191 for $\delta^2\text{H}$, with LOCEAN data been lower than $\delta^2\text{H}$ from Bonne et al. (2019) by $0.99 \pm$
192 0.07 ‰ (Fig. 1d, e).

193

194 2.2 Southern subtropical Indian Ocean

195 [Glaubke et al. \(GWS2024\)](#) describe a synthesis of water isotope data in the southern
196 Indian Ocean combining their [new dataset data collected in 2018](#) in the southeastern
197 Indian Ocean (CROCCA-2S) with earlier data in the south-western Indian Ocean, in
198 particular from LOCEAN, as well as data from the [southern](#) Australian shelf collected
199 mostly in 2010 (Richardson et al., 2019), and in the equatorial Indian Ocean (Kim et al.,
200 2021). In the most recent version of the LOCEAN data-set, in addition to data included ~~in~~
201 [by Glaubke et al. \(GWS2024\) for comparison and and](#) collected mostly west of 80°E ,
202 there are two transects with surface data through the southeastern Indian Ocean, one
203 collected in February 2017, and the other in March 2024, thus in mid to late austral
204 summer. These transects cross the region covered by the CROCCA-2S data-set, albeit not
205 close to [western](#) Australia, as well as the area of the Richardson et al. (2019) data-set,
206 south of Australia. The LOCEAN data-set also contains surface data south of Tasmania (in
207 2017, as well as in 2020 to 2024). All these data correspond to samples analyzed on a
208 CRDS Picarro L2130 at LOCEAN, and with the protocols discussed [by](#) ~~in~~ Reverdin et al.
209 (2022). The bottles in which the samples were stored were the same [ones](#) for [all-most of](#)
210 the samples, and time between collection and analysis varied, but was mostly on the
211 order of 6 months or less. Thus, this is a homogeneously produced set of data ~~in~~ for the
212 years 2016-2024, which spatially and temporally overlaps with the data used ~~in-by~~
213 [Glaubke et al. \(GWS2024\)](#) collected south of Australia and in the southeastern Indian
214 Ocean (Fig. 2).



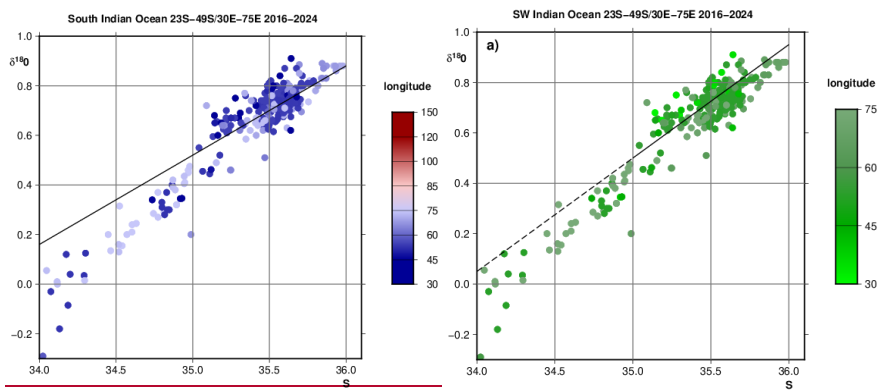
215
216

217 Figure 2: Map of $\delta^{18}\text{O}$ surface data in the LOCEAN archive for 2016-2024, north of 60°S .
218 All ~~these~~ data are associated with S and $\delta^2\text{H}$ ~~datameasurements~~.

219 The LOCEAN data distribution ~~indicates some scatter in~~plotted in the S- $\delta^{18}\text{O}$ ~~space~~
220 ~~presents a wide $\delta^{18}\text{O}$ distribution range at a given salinity~~ in the southwestern Indian
221 Ocean (Fig. 3a) for S ~~larger than 35~~between 35 and 36. For this range which covers a
222 large part of the surface water of the southwestern Indian Ocean's subtropical gyre, we
223 establish a regression line for the LOCEAN $\delta^{18}\text{O}$ as a function of S, which can be seen as a
224 mixing line. Above this line, there are no data points for lower S (Fig. 3a), with data at
225 higher S. Data above the regression line on Fig. 3a, established for all data with S
226 between 35 and 36, are present only for S larger than 35.0, and are found north of 28°S
227 and as well as in the far south-western Indian Ocean, but with some remnants found all
228 the way to the core of the subtropical gyre near $75^\circ\text{E}/35^\circ\text{S}$ (Fig. 3b). Data below the
229 regression line contain most of the data ~~east of 60°E for latitudes~~ south of 28°S and ~~east~~
230 ~~of 60°E and~~ connect the salinity maximum region with the lower salinity south of the
231 Subtropical Front and down to the region south of the Polar Front (Fig. 3c). These

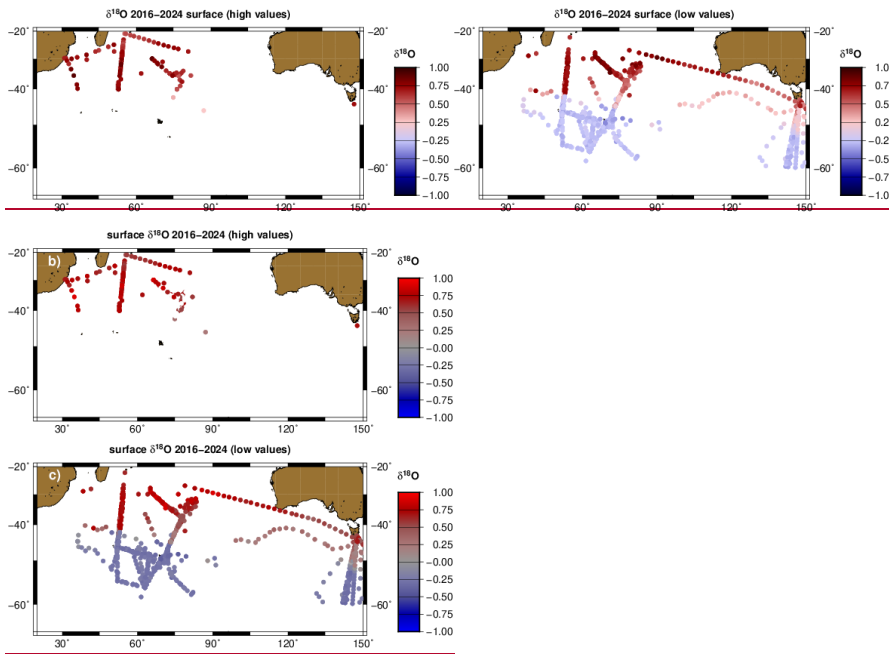
232 subtropical lower isotopic values in S- $\delta^{18}\text{O}$ space, which already appear in part of the the
 233 repeated (1998-2024) French OISO cruises data (in 1998-2024) at 50°E, albeit not all
 234 the time, dominate east of 60°E.

235 a)



236

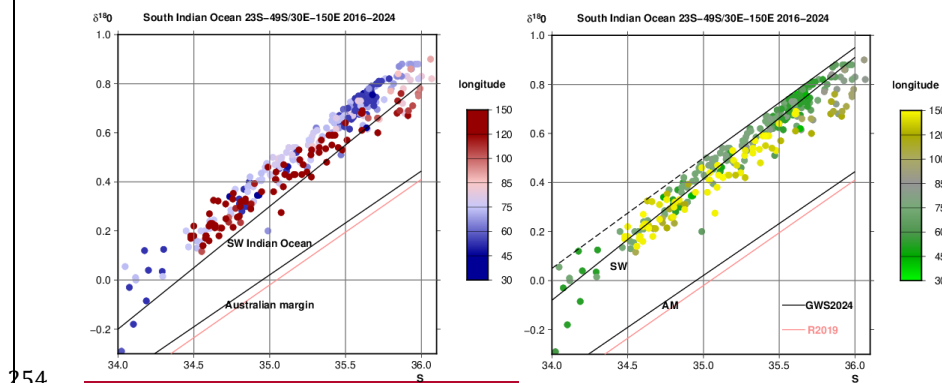
237 b) ————— c)



239

240 Figure 3: (a) S - $\delta^{18}\text{O}$ scatter diagram of $(S, \delta^{18}\text{O})$ 0-30m LOCEAN data within the
 241 southwestern region (30-75°E/23-49°S) coloured as a function of longitude, with the
 242 regression line (black line) of the data having an S - $\delta^{18}\text{O}$ practical space for the 35-36
 243 range in practical salinity between 35 and 36 (black line) overlaid. The spatial
 244 distributions of the LOCEAN data with higher and lower $\delta^{18}\text{O}$ relative to that regression
 245 line in the whole Indian Ocean north of 60°S are shown on panels (b) and (c),
 246 respectively.

247 When focusing We will now focus on the lower part of the distribution in S - $\delta^{18}\text{O}$ space
 248 (Fig. 3c), which overlaps with the location of the data from CROCCA-2S and the near-
 249 Australia data from GWS2024 (the higher values in Fig. 3c do not). For salinities above
 250 35, one observes a gradual lowering of $\delta^{18}\text{O}$ at given salinity from west to east 50°E in
 251 the western Indian Ocean to at least 100°E for salinities above 35 (Fig. 4) all the way to
 252 150° with more stable values further east. This lowering is on the order of 0.15 at most,
 253 even for the higher salinities (35.5 or more) for which it is strongest. (Fig. 4).



254
 255 Figure 4: The S - $\delta^{18}\text{O}$ scatter plot of 0-30m LOCEAN Indian Ocean data as shown in Fig.
 256 3c, color-coded as a function of longitude, below the partially stippled regression
 257 line for the SW Indian Ocean (of reproduced from Fig. 3a) (the ones mapped in Fig. 3c)
 258 in S - $\delta^{18}\text{O}$ space, color-coded as a function of longitude. The two black lines correspond to
 259 the two linear relationships (GWS2024) for the 0-100m layer recommended in this
 260 region between 23°S and 49°S by Glaubke et al. (2024) for the south-west Indian Ocean
 261 (SW) and for the Australian margin (south of Australia (AM)) (we use the original

262 relation $\delta^{18}\text{O} = 0.4231 * S - 14.7876$, instead of the rounded-up relation reported in
 263 the paper; R. H. Glaubke, pers. comm., 2024), ~~and the pink line is -are also plotted (black~~
 264 ~~lines), as well as~~ the earlier linear relationship for the 0-600m layer along the
 265 Australian margin by Richardson et al. (2019) (R2019 in pink).

Mis en forme : Anglais (États-Unis)

266
 267 Thus, besides some gradual and smaller changes, we do not observe in the LOCEAN
 268 surface dataset a large sudden change in the $\{S, \delta^{18}\text{O}\}$ distribution near 75°E or 85°E
 269 between the southeastern and southwestern Indian Ocean, nor a further strong change
 270 closer to the Australian coastal margin, as suggested by figures 6 and 7 of Glaubke et al.
 271 (GWS2024). Most of the LOCEAN $\{S, \delta^{18}\text{O}\}$ data south of 28°S correspond to the mixing
 272 of a low salinity end-member characteristic of the fresh waters of the Southern Ocean
 273 (at $S < 34$) with waters which are imprinted by air-sea exchange ~~of water in a wider~~
 274 ~~range of values at the subtropical gyre at higher salinities up to $S \rightarrow 36.36$ and more,~~ as
 275 discussed ~~by~~ in Glaubke et al. (GWS2024). These LOCEAN $(S, \delta^{18}\text{O})$ values are
 276 significantly above the linear relationships proposed by Glaubke et al. (GWS2024 ~~(based~~
 277 ~~on their figures 5a, 6 and 7)~~). This positive offset ~~at given S~~ seems to be about ~~0.1505-~~
 278 ~~0.10~~ ‰ in the southwestern Indian Ocean, but close to 0.50 ‰ for the Australian
 279 coastal margins, although we could not access the individual data ~~of for that latter~~
 280 ~~region R2019 for that latter region~~. These offsets are much larger than the ~~scatter~~
 281 ~~presentspread~~ in the LOCEAN data, which is ~~on~~ the order of 0.10 ‰. Furthermore, the
 282 LOCEAN data support the presence of a secondary low salinity end member at $S < 35$
 283 with heavier isotopic composition, contributing to the water ~~r- ρ~~ mass properties in the far
 284 southwestern Indian Ocean as well as for the area sampled between 20°S and 28°S north
 285 of the subtropical salinity maximum. This could be a contribution of the Indonesian
 286 Through Flow and tropical western Indian Ocean surface waters, as discussed by Kim et
 287 al. (2021) and Glaubke et al. (GWS2024). We could not carry out a comparable
 288 comparison for $\delta^2\text{H}$ which is not presented ~~in by~~ Glaubke et al. (GWS2024), and which
 289 exhibits a too large ~~scatter spread~~ in the CROCCA-2S data-set to reach a firm conclusion.

290 3. Discussion

291 In the two [inter](#)comparisons of surface data presented in this note, we find significant
292 ~~differences~~[differences between datasets](#). Do these differences originate from spatio-
293 temporal variability or from systematic offsets [between the different datasets](#)?

294 In the case of the RV Polarstern dataset (Bonne et al., 2019), an error in a specified
295 reference material value was found after the publication, and the adjusted data present
296 only a small, non-significant $\delta^{18}\text{O}$ negative offset, but a significant positive $\delta^2\text{H}$ offset
297 with respect to LOCEAN data. Differences might arise from spatial differences. For
298 example, in the northern hemisphere, values at salinity close to 35 ~~psu~~ mostly originate
299 from the North Sea and English Channel in the [RV Polarstern](#) dataset, thus with more
300 mid-latitude continental influence than for most of the LOCEAN data in the same salinity
301 range which have a contribution of more depleted subpolar and polar freshwater. One
302 expects a larger [scatter isotopic range](#) in the South Atlantic for salinities less than 35,
303 due to intermittent presence of sea ice or iceberg melt, and at higher salinities due to the
304 presence of different water masses originating from the South Atlantic and southeastern
305 Indian Ocean. However, the current data-set is not sufficient to estimate it.

306 Furthermore, different seasons were sampled in the two datasets. In the northeastern
307 Atlantic sector, Bonne et al. (2019) surface data east of 30°W were collected in April and
308 November north of 10°S and in November south of 10°S in the southeastern Atlantic.
309 These data do not suggest large seasonal differences in the Northeast Atlantic,
310 concurring with the LOCEAN (~~S- $\delta^{18}\text{O}$~~) data in the tropics to mid-latitudes (20 to 50°N),
311 which are tightly distributed along a mean S- $\delta^{18}\text{O}$ relationship, and thus with low
312 seasonal variability [of this relationship](#) (Benetti et al., 2017a; Voelker et al., 2015). The
313 LOCEAN data are not numerous enough in the ~~s~~[South-Eastern](#) Atlantic to further
314 evaluate whether the offset is constant throughout the data-set, or presents a
315 component related to geographical temporal or spatial variability.

316 To investigate the South Indian Ocean sea-water isotopic composition, [Glaubke et al.](#)
317 ~~(GWS2024)~~ combined data-sets that were processed in different ~~institutes~~[laboratories](#).
318 Potential offsets between those could thus cause apparent spatial variability. In
319 particular, [Glaubke et al. \(GWS2024\)](#) outline large spatial contrasts in the S- $\delta^{18}\text{O}$
320 relationship across the surface subtropical Indian Ocean and southern Australia that are
321 at least a factor two smaller in the recent version of the LOCEAN ~~database~~[dataset](#).

322 Seasonal or interannual variability might contribute to the differences shown on Fig. 3,
323 as the data in the southeastern Indian Ocean from [Glaubke et al. \(GWS2024\)](#) were
324 collected in November-December, whereas the data in the LOCEAN database in this
325 region are mostly from February-March. However, at least south of Tasmania, where the
326 LOCEAN [data base dataset](#) also contains December data, it does not seem that the
327 seasonal cycle causes [differences-changes](#) larger than 0.05 ‰ at the same salinity. A
328 difference due to seasonality would thus be barely identifiable in that case, noting the
329 possible presence of interannual variability and that the long-term accuracy in the
330 analyses in some centers, such as AWI Potsdam and LOCEAN, is 0.05 ‰. Richardson et
331 al. (2019) also commented that south of Australia there was little difference between a
332 southern winter cruise and late summer (March) data. Further west, near 55-70°E,
333 earlier surface data in the OISO surveys, as well as the vertical upper profiles of OISO
334 station data also suggest a rather modest seasonal variability on the order of 0.10 ‰.
335 Changes could also arise from interannual variability, but the range of interannual
336 variability in the LOCEAN data base is smaller than the difference between the [Glaubke](#)
337 [et al \(GWS2024\)](#) curves for the southeastern Indian Ocean and south of Australia and
338 the corresponding LOCEAN data. Thus, a likely cause of the large differences between
339 the South Indian Ocean/Australia margin data combined in the [Glaubke et al.](#)
340 [\(GWS2024\)](#) study is the existence of systematic offsets between the data produced ~~in~~-by
341 different institutes.

342 4. Conclusions

343 What these two comparisons suggest is that offsets are present between different recent
344 [published](#) data-sets ~~published~~, which exceed 0.10 ‰ in $\delta^{18}\text{O}$ and 0.50 ‰ in $\delta^2\text{H}$, thus
345 larger than the target long-term accuracy of analyses in individual isotopic laboratories.
346 Moreover, errors in reference material values are always possible and require post-
347 analysis intercomparisons, such as the one that led to the correction of the RV
348 Polarstern [Bonne et al. \(2019\)](#) data-set ([Bonne et al., 2019](#)). Furthermore, one
349 contribution to a systematic difference between the LOCEAN data-set and data from
350 other institutes is that the LOCEAN data are reported in 'freshwater' concentration scale
351 (Benetti et al., 2017b). The use of this concentration scale corrects possible effects of salt
352 in the water activity measured by IRMS with CO_2 -equilibration and the effect of salt
353 accumulation during evaporation in laser spectroscopy, which both can lead to

Mis en forme : Police :Couleur de police : Noir,
Anglais (États-Unis)

354 fractionation, possibly of similar magnitude (Walker et al., 2016). Different comparisons
355 based on duplicates collected during cruises suggest that this is a main cause of
356 difference between LOCEAN data and other data-sets (LOCEAN $\delta^{18}\text{O}$ data being ~~ingen~~ more
357 positive). Poor conservation of the samples during storage, analytical protocols, or
358 uncertainties in the specified values of reference material are other sources of
359 differences between data produced in different institutes.

360 ~~The methods~~Different methods have been used for intercomparing and detecting
361 systematic offsets between different data-sets ~~are not numerous. On one hand, one~~
362 ~~could~~One common approach is to compare values obtained in specific water masses, for
363 which we expect little variability of the water isotopic composition. This is often
364 ~~used~~attempted, but ~~such data are not always available~~data density is often limited, and
365 the resulting uncertainties are difficult to assess, ~~although data~~. Data-sets with
366 intermediate and deep data in the Southern Ocean might be ~~used~~valuable to
367 systematically test this approach, and model-based reconstructions of isotopic
368 composition of sea water could also be incorporated. One could also develop

369
370 An alternative, in particular for the surface data, is to develop approaches ~~a method~~
371 based on the systematic comparison of nearby data in space and time, as. ~~In some ways,~~
372 the assumption behind this and what was done in the mapping by LeGrande and
373 Schmidt (2006), that is that the bulk of the variability is from large scale relationships of
374 water isotopes and salinity. -is suggested in Fig. 1 when ~~This is also what has been done~~
375 by crossover analyses in major geochemical databases, such as GLODAP, with an
376 attempt to adjust offsets for $\delta^{13}\text{C}$ -DIC with a similar low-density data distribution in the
377 North Atlantic (Becker et al., 2016). The ~~comparing~~ comparison presented here (Fig. 1)
378 of the S-water isotopes surface distribution in the North and South Atlantic ~~in~~ of the
379 LOCEAN and the RV Polarstern (Bonne et al., 2019) data-sets suggests that this can be
380 used to estimate offsets. This could be further improved ~~Required improvements, in~~
381 particular for estimating uncertainties would be to take into account estimates of
382 seasonal, interannual and spatial variability in these relationships, but. ~~However, this~~
383 requires that there are enough overlapping data within regions of relatively
384 homogeneous ~~signals~~water masses, or some independent estimates on these signals, for
385 example from model simulations.

386

387 As the spatial and temporal data density is ~~not always often reduced sufficient~~, these
 388 ~~approaches may fail~~ we expect that the uncertainties in estimated offsets will be large.
 389 This could reduce the usefulness of the isotopic data for different oceanographic and
 390 climate studies, with large uncertainties in estimated S- $\delta^{18}\text{O}$ (or S- $\delta^2\text{H}$) relationships to
 391 validate proxies used for paleo-climate reconstructions, or for identifying emerging
 392 climate-change related signals.

393

394 Scientific Committee of Oceanic Research (SCOR) working group 171 MASIS (Towards
 395 best practices for Measuring and Archiving Stable Isotopes in Seawater) has recently
 396 been established to contribute tackling these issues, both for water isotopes and the
 397 isotopic composition of inorganic carbon in sea water, $\delta^{13}\text{C-DIC}$. For that, it aims to
 398 actively involve the international community in establishing guidelines for data
 399 production (collection, storage, measurement) and quality control, as well as for
 400 validating the data and comparing well-documented archived data originating from
 401 different laboratories. It will review the methods to estimate errors and offsets between
 402 the different datasets. Thus, An important step for this effort is to directly intercompare
 403 measurements by the different laboratories - an important complementary approach is
 404 to ~~of actively share~~ well-preserved water samples, distributed quickly, and
 405 dedicated to specific intercomparison of data produced in the different laboratories,
 406 building on previous efforts as had earlier been done for $\delta^{13}\text{C-DIC}$ (Cheng et al., 2019).
 407 This, together with ~~establishing well-accepted guidelines for data production and quality~~
 408 ~~control, and enhancing scientific interaction~~ exchange between the different
 409 ~~institutes~~ within the scientific community needs to be actively pursued, in order to
 410 reduce the errors when merging different datasets and increase the potential use of the
 411 water isotope data, ~~as EOJ/ECCVs. This approach is recommended by the recently~~
 412 ~~established working group MASIS (Towards best practices for Measuring and Archiving~~
 413 ~~Stable Isotopes in Seawater) of the Scientific Committee of Oceanic Research (SCOR).~~
 414 Without such direct intercomparison of samples, the usefulness of the isotopic data for
 415 different oceanographic and climate studies is strongly reduced, for example resulting in
 416 large uncertainties when establishing different S- $\delta^{18}\text{O}$ (or S- $\delta^2\text{H}$) relationships to
 417 validate studies of proxies to support paleo-climate reconstructions.

418

Mis en forme : Police :+Corps (Cambria)

Mis en forme : Police :+Corps (Cambria)

Mis en forme : Police :+Corps (Cambria), Non

Mis en forme : Police :+Corps (Cambria)

Mis en forme : Police :+Corps (Cambria), Non

Mis en forme : Police :+Corps (Cambria)

Mis en forme : Police :+Corps (Cambria), Non

Mis en forme : Police :+Corps (Cambria)

Mis en forme : Police :+Corps (Cambria), Non

Mis en forme : Police :+Corps (Cambria)

Mis en forme : Police :+Corps (Cambria), Non

Mis en forme : Police :+Corps (Cambria)

Mis en forme : Police :+Corps (Cambria)

Mis en forme : Police :+Corps (Cambria)

419 Data availability

420 The LOCEAN data are available at <https://www.seanoe.org/data/00600/71186/>.
421 The isotopic data of the Bonne et al. (2019) are available as indicated in the paper, with
422 here S added from the PANGAEA archive, as described in the text. The ~~Glaubke et al.~~
423 ~~(GWS20244)~~ data are available as described in the paper. However, among the data
424 used in this paper, we could not access the data from the Richardson et al. (2019) paper.

Code de champ modifié

425
426 Author contribution: GR initiated the study and prepared the manuscript with
427 contributions from all coauthors. AV initiated the intercomparison effort, and AV, CW,
428 and HM contributed to editing the paper. HM was also responsible from producing the
429 data in the Bonne et al. (2019) paper.

430
431 Competing interests: The authors declare that they have no conflict of interest.

432
433 Acknowledgments

434 The LOCEAN isotopic laboratory is supported by OSU Ecce Terra of Sorbonne Université.
435 We are thankful to Catherine Pierre and Jérôme Demange who have set and help run the
436 facility, and for Aïcha Naamar, Marion Benetti and Camille Akhoudas to have measured
437 some of the water samples. We are grateful for support by INSU, Nicolas Metzl and Claire
438 Lo Monaco for samples during the OISO cruises on RV MD2, by IPEV during the SOCISSE
439 program on RV Astrolabe, with on board support by Patrice Bretel and Rémi Foletto, and
440 by IPSL for supporting the LOCEAN data base and intercomparisons. Antje Voelker
441 thanks Joanna Waniek (IOW, Germany) for collecting the NE Atlantic water samples and
442 Robert van Geldern (GeoZentrum Nordbayern, Germany) for analyzing them. ~~She,~~
443 ~~also,AV also~~ acknowledges financial support by Fundação para a Ciência e a Tecnologia
444 (FCT) through projects Centro de Ciências do Mar do Algarve (CCMAR) basic funding
445 UIDB/04326/2020 (<https://doi.org/10.54499/UIDB/04326/2020>) and programmatic
446 funding UIDP/04326/2020 (<https://doi.org/10.54499/UIDP/04326/2020>) and the
447 CIMAR associated laboratory funding LA/P/0101/2020
448 (<https://doi.org/10.54499/LA/P/0101/2020>). The RV Polarstern data-set was funded
449 by the AWI Strategy Fund Project ISOARC. Comments by Alexander Haumann (AWI) and
450 by two anonymous reviewers were very helpful.

Code de champ modifié

Code de champ modifié

452 References

- 453 Aoki, S., Kobayashi, R., Rintoul, S. R., et al.: Changes in water properties and flow regime
454 on the continental shelf off the Adélie/George V Land coast, East Antarctica, after glacier
455 tongue calving, *J. Geophys. Res.: Oceans*, 122, 6277-6294, 2017.
- 456 Akhoudas, C. H., Sallée, J.-B., Haumann, F. A., Meredith, M. P., Garabato, A. N., Reverdin,
457 G., Jullion, L., Aloisi, G., Benetti, M., Leng, M. J., and Arrowsmith, C.: Ventilation of the
458 abyss in the Atlantic sector of the Southern Ocean, *Nature scientific reports*, **11**, 16733,
459 <https://doi.org/10.1038/s41598-021-95949-w>, 2020, 2021.
- 460 Atwood, A. R., Moore, A.L., Long, S., Pauly, R., DeLong, K., Wagner, A., and Hargreaves, J.A.:
461 The CoralHydro2k Seawater $\delta^{18}\text{O}$ Database, *Past Global Changes Magazine* 32,59, doi:
462 10.22498/pages.32.1.59, 2024.
- 463 [Becker, M., Andersen, N., Erlenkeuser, H., Tanhua, T., Humphreys, M.P., and Körtzinger, A.:](#)
464 [An Internally Consistent Dataset of \$\delta^{13}\text{C}\$ -DIC Data in the North Atlantic Ocean. *Earth Sys.*](#)
465 [Sci. Data, 8, 559-570, doi: 10.5194/essd-8-559-2016, 2016.](#)
- 466 Benetti, M., Reverdin, G., Aloisi, G., and Sveinbjörnsdóttir, A.: Stable isotopes in surface
467 waters of the Atlantic Ocean: indicators of ocean-atmosphere water fluxes and oceanic
468 mixing processes. *J. Geophys. Res. Oceans*, doi:10.1002/2017JC012712, 2017a.
- 469 Benetti, M., Sveinbjörnsdóttir, A. E., Ólafsdóttir, R., Leng, M. J., Arrowsmith, C., Debondt,
470 K., Fripiat, F., and Aloisi, G.: Inter-comparison of salt effect correction for $\delta^{18}\text{O}$ and $\delta^2\text{H}$
471 measurements in seawater by CRDS and IRMS using the gas-H₂O equilibration method,
472 *Marine chemistry*, doi:10.1016/j.marchem.2017.05.010, 2017b.
- 473 Biddle, L. C., Loose, B., and Heywood, K. J.: Upper ocean distribution of glacial meltwater
474 in the Amundsen Sea, Antarctica. *J. Geophys. Res. Oceans*, 10.1029/2019JC015133. et al.,
475 2019.
- 476 Bonne, J.-L., Behrens, M. Meyer, H., Kipfstuhl, S., Rabe, B., Schönicke, L., Steen-Larsen, H.
477 C., Werner, M.: Resolving the controls of water vapour isotopes in the Atlantic sector.
478 *Nature Comm.* 10, 1632, doi: 10.1038/s41467-019-09242-6, 2017.
- 479 Boutin, J., Chao, Y., Asher, W. E., Delcroix, T., Drucker, D., et al.: Satellite and In Situ
480 Salinity: Understanding Near-Surface Stratification and Subfootprint Variability. *Bull. of*
481 *the Amer. Meteor. Soc.*, 97 (8), pp.1391-1407. 10.1175/BAMS-D-15-00032.1, 2016.
- 482 Brady, E., Stevenson, S., Bailey, D., Liu, Z., Noone, D., Nusbaumer, J., Otto-Bliesner, B. L.,
483 Tabor, C., Thomas, R., Wong, T., Zhang, J., Zhu, J.: The connected isotopic water cycle in

Code de champ modifié

Code de champ modifié

484 the Community Earth System Model Version 1, *J. Adv. Model. Earth Syst.*, 11, 8,
485 <https://doi.org/10.1029/2019MS001663>, 2019.
486 Cauquoin, A., Werner, M., Lohmann, G.: Water isotopes – climate relationships for the
487 mid-holocene and preindustrial period simulated with an isotope-enabled version of
488 MPI-ESM, *Clim. Past* 15, 1913-1937, <https://doi.org/10.5194/cp-15-1913-2019>, 2019.

489 Cheng, L., Normandeau, C., Bowden, R., Doucett, R., Gallagher, B., Gillikin, D. P.,
490 Kumamoto, Y., McKay, J. L., Middlestead, P., Ninnemann, U., Nothaft, D., Dubinina, E. O.,
491 Quay, P., Reverdin, G., Shirai, K., Mørkved, P. T., Theiling, B.P., van Geldern, R., and
492 Wallace, D. W. R.: An international intercomparison of stable carbon isotope
493 composition measurements of dissolved inorganic carbon in seawater, *Limnology and*
494 *Oceanography: Methods* 17, 200-209, <https://doi.org/10.1002/lom3.10300>, 2019.

Code de champ modifié

495 Glaubke, R. H., Wagner, A., and Sikes, E. L.: Characterizing the stable oxygen isotopic
496 composition of the southeast Indian Ocean, *Marine Chemistry*, 262,
497 <https://doi.org/10.1016/j.marchem.2024.104397>, 2024.

Code de champ modifié

498 Haumann, F. A. et al.: [Data set], Zenodo, doi:10.5281/zenodo.1494915, 2019.
499 Hennig, A., Mucciarone, D. A., Jacobs, S. S., Mortlock, R. A., and Dunbar, R. B.: Meteoric
500 water and glacial meltwater in the southeastern Amundsen Sea: a time series from 1994
501 to 2020, *The cryosphere*, 18, 791-818, <https://doi.org/10.519/tc-18-791-2024>, 2024.

Code de champ modifié

502 Hilaire-Marcel, C., Kim, S. T., Landais, A., Ghosh, P., Assonov, S., Lécuyer, C., Blanchard, M.,
503 Meijer, H. A., and Steen-Larsen, H. C.: A stable isotope toolbox for water and inorganic
504 carbon cycle studies, *Nature Reviews Earth & Environment* 2 (10), 699-719, 2021.
505 Kim, Y., Rho, T., and Kang, D.-J.: Oxygen isotope composition of seawater and salinity in
506 the western Indian Ocean: Implications for water mass mixing, *Mar. Chem.* 237, 104035,
507 <https://doi.org/10.1016/j.marchem.2021.104035>, 2021.

Code de champ modifié

508 Konecky, B. L. et al.: The Iso2k database: a global compilation of paleo- $\delta^{18}\text{O}$ and $\delta^2\text{H}$
509 records to aid understanding of Common Era climate, *Earth Syst. Sci. Data*, 12, 2261–
510 2288, <https://doi.org/10.5194/essd-12-2261-2020>, 2020.

511 Kumar, P. K., Singh, A., and Ramesh, R.: Convective mixing and transport of the Bay of
512 Bengal water stir the $\delta^{18}\text{O}$ -salinity relation in the Arabian Sea, *J. Mar. Sys.* 238, 103842,
513 <https://doi.org/10.1016/j.jmarsys.2022.103842>, 2023.

Code de champ modifié

- 514 LeGrande, A. N. and Schmidt, G. A.: Global gridded data set of the oxygen isotopic
515 composition in seawater, *Geophys. Res. Lett.* 33,
516 <https://doi.org/10.1029/2006gl026011>, 2006.
- 517 Oppo, D. W., Schmidt, G. A., and LeGrande, A. N.: Seawater isotope constraints on tropical
518 hydrology during the Holocene, *Geophys. Res. Lett.* 34, L13701,
519 <https://doi.org/10.1029/2007GL030017>, 2007.
- 520 Randall-Goodwin, E., Meredith, M. P., Jenkins, A., Yager, P. L., Sherrell, R. M., Abrahamsen,
521 E. P., Guerrero, R., Yuan, X., Mortlock, R. A., Gavahan, K., Alderkamp, A.-C., Ducklow, H.,
522 Robertson, R., and Stammerjohn, S. E.: Freshwater distributions and water mass
523 structure in the Amundsen Sea polynya region, Antarctica. *Elementa: Science of the*
524 *Anthropocene*, 3: 000065, <https://doi.org/10.12952/journal.elementa.000065>, 2015.
525 et al., 2015.
- 526 Reverdin, G., et al.: The CISE-LOCEAN sea water isotopic database (1998-2021), *Earth*
527 *sci. sys. data*, <https://doi.org/10.5194/essd-2022-34>, 2022.
- 528 Richardson, L. E., Middleton, J. F., Kyser, T. K., James, N. P., and Opdyke, B. N.: Shallow
529 water masses and their connectivity along the southern Australian continental margin,
530 *Deep Sea Res. I, Oceanogr. Res. Pap.* 152, 103083,
531 <http://doi.org/10.1016/j.dsr.2019.103083>, 2019.
- 532 Schmidt, G. A., LeGrande, A. N., and Hoffmann, G.: Water isotope expressions of intrinsic
533 and forced variability in a coupled ocean-atmosphere model, *J. Geophys. Res.* 112,
534 D10103, <https://doi.org/10.1029/2006jd007781>, 2007.
- 535 Voelker, A., Colman, A., Olack, G., Waniek, J. J., and Hodell, D.: Oxygen and hydrogen
536 isotope signatures of Northeast Atlantic water masses, *Deep-Sea Res. II*, 116, 89-106.
537 <https://doi.org/10.1016/j.dsr2.2014.11.006>, 2015.
- 538 Voelker, A. H.: Seawater oxygen and hydrogen stable isotope data from the upper water
539 column in the North Atlantic Ocean (unpublished data). *Interdisciplinary Earth Data*
540 *Alliance (IEDA)*, <https://doi.org/10.26022/IEDA/112743>, 2023.
- 541 Walker, S. A., Azetsu-Scott, K., Normandeau, C., Kelly, D. E., Friedrich, R., Newton, R.,
542 Schlosser, P., McKay, J. L. Abdi, W., Kerrigan, E., Craig, S. E., and Wallace, D. W. R.: Oxygen
543 isotope measurement of seawater ($H_2^{18}O/H_2^{16}O$). A comparison of cavity ring-down
544 spectroscopy (CRDS) and isotope ratio mass spectrometry (IRMS), *Limnol. and*
545 *Oceanography: Methods*, 14, 31-38, <https://doi.org/10.1002/lom3.10067>, 2016.

Code de champ modifié

Code de champ modifié

Code de champ modifié

Code de champ modifié

Code de champ modifié

Code de champ modifié